Proceedings of the 2006 American Control Conference
Minneapolis, Minnesota, USA, June 14-16, 2006

Turbulence suppression in channel flows by small amplitude transverse wall oscillations

Mihailo R. Jovanović

Abstract— **We model and analyze the influence of small amplitude transverse wall oscillations on the evolution of velocity perturbations in channel flows. The amplitude and frequency of periodic oscillations enter as coefficients, and spatially distributed and temporally varying body force fields enter as stochastic external excitations to our models. We quantify the effect of these excitations on velocity perturbation energy and develop a system theoretic paradigm for the optimal selection of transverse oscillation parameters for turbulence suppression. We use a perturbation analysis to demonstrate that depending on the wall oscillation frequency the energy of velocity perturbations can be increased or decreased compared to the uncontrolled flow. Our results provide a first compelling theoretical explanation as to why properly designed transverse wall oscillations can suppress turbulence in the wall-bounded shear flows.**

I. Introduction

Turbulence suppression by sensorless mechanisms is a promising technology for implementation, as it represents a much simpler alternative to feedback flow control with wall-mounted arrays of sensors and actuators. Examples of sensorless strategies include: transverse wall oscillations, control of conductive fluids using the Lorentz force, and wall geometry deformation such as riblets. Although several numerical and experimental investigations indicate that *properly designed* sensorless strategies can lead to a significant drag reduction, an obstacle to fully utilizing these approaches is the absence of a theoretical framework for their design, optimization, and evaluation. This lack of analytical tools greatly impedes the design and optimization of sensorless schemes as well as their extension to different flow regimes.

Skin-friction drag reduction by means of transverse oscillations was first explored in [1]. The direct numerical simulations of a turbulent channel flow subject to either a spanwise oscillatory wall motion or an oscillatory spanwise body force showed that a substantial drag reduction (up to $40\,\%$) can be achieved for certain values of oscillation frequency. The attenuation of velocity fluctuations (up to $30\,\%$) was also reported. These observations served as a motivation for further numerical and experimental studies in channel [2]–[4], pipe [5]–[7], and boundary layer [8]–[10] flows.

In this paper, we model and analyze the influence of transverse wall oscillations on the evolution of velocity perturbations in *transitional channel flows*. Our results complement previously reported numerical and experimental studies [1]–[10], and furnish a theoretical framework for design of efficient turbulence suppression strategies. Since the transition in channel flows is not appropriately described by the eigenvalue analysis [11]–[17], we perform an input-output analysis of stochastically excited linearized Navier-Stokes (NS) equations. Our analysis quantifies the effect of body force fields on velocity perturbations and provides a system theoretic paradigm for the optimal selection of transverse oscillation parameters for turbulence suppression.

Our presentation is organized as follows: in section II we determine nominal velocity of the channel flow subject to transverse wall oscillations, and give dynamical description of the flow fluctuations evolving around this velocity profile. In § III, we introduce a notion of the *frequency response* of linear time-periodic (LTP) systems and present a computationally efficient method for determination of the $\mathcal{H}_2$ norm in the presence of small amplitude oscillations. In § IV, we employ perturbation analysis to identify the oscillation frequency that leads to the largest $\mathcal{H}_2$ norm reduction for streamwise constant perturbations. We also derive an explicit dependence of the $\mathcal{H}_2$ norm on the Reynolds number R. In § V, we summarize the major contributions.

II. Dynamics of velocity fluctuations

A. Nominal velocity

Consider a flow between two parallel infinite plates with geometry illustrated in Fig. 1. Incompressible flow of a viscous Newtonian fluid satisfies the NS equations and the continuity equation given in their non-dimensional forms by

$$\begin{aligned} \mathbf{u}_t &= -\ _{\mathbf{u}}\mathbf{u} - \quad P + (1/R)\Delta\mathbf{u} + \mathbf{F}, \\ 0 &= \quad \cdot\mathbf{u}, \end{aligned} \tag{1}$$

where $\mathbf{u}$ is the velocity vector, P is the pressure, $\mathbf{F}$ is the body force, $\quad$ is the gradient, $\Delta := \quad^2$ is the Laplacian, and operator $_{\mathbf{u}}$ is defined as $_{\mathbf{u}} := \mathbf{u}\cdot\quad$. The Reynolds number is defined in terms of centerline velocity $\bar{U}$ and channel half-width δ, $R := \bar{U}\delta/\nu$, where ν denotes the kinematic viscosity.

Let the flow be subject to a transverse oscillation of the lower-wall, and let the nominal body force be equal to zero, $\bar{\mathbf{F}} \equiv 0$. Due to no-slip, the wall oscillation imposes an oscillatory boundary condition on the spanwise component of nominal velocity $\bar{\mathbf{u}} := \begin{bmatrix} U & V & W \end{bmatrix}^T$. If the upper wall is fixed, and if the lower wall oscillates with frequency $\omega_o := 2\pi/T$, the nominal velocity can be determined from (1) subject to

$$\begin{aligned} &W(-1) := 2\alpha \sin \omega_o t, \quad \bar{P}_x = -2/R, \quad \bar{\mathbf{F}} \equiv 0, \\ &U(\pm 1) = 0, \quad V(\pm 1) = V_y(\pm 1) = W(1) = 0, \end{aligned} \tag{2}$$

where positive parameters α and T, respectively, denote the non-dimensional amplitude and period of wall oscillations.

M. R. Jovanović is with the Department of Electrical and Computer Engineering, University of Minnesota, Minneapolis, MN 55455, USA (e-mail: mihailo@umn.edu).

1-4244-0210-7/06/$20.00 ©2006 IEEE

If W_w and T_w are the wall oscillation amplitude and period in physical units, then $\alpha := W_w/\bar{U} = R_w/R$ and $T := T_w/T_c$, where $R_w := W_w\delta/\nu$ is the Reynolds number defined in terms of W_w, and $T_c := \delta/\bar{U}$ is the convective time-scale. The amplitude of wall oscillations is multiplied by two for a convenience of later algebraic manipulations.

In the steady-state (1) simplifies to the x and z-direction momentum equations

$$0 = -\bar{P}_x + (1/R)U_{yy}, \tag{3a}$$
$$W_t = (1/R)W_{yy}. \tag{3b}$$

The steady-state solution to (3,2) is given by $\bar{\mathbf{u}} := \begin{bmatrix} U(y) & 0 & W(y,t) \end{bmatrix}^T$, where $U(y) = 1-y^2$ denotes the Poiseuille flow, and

$$W(y,t) = 2\alpha\,(W_c(y)\cos\,\omega_o t + W_s(y)\sin\,\omega_o t)\,.$$

Functions $W_c(y)$ and $W_s(y)$ represent solutions to the following two point boundary value problem (TPBVP):

$$W_s''(y) = -\Omega W_c(y), \qquad W_c''(y) = \Omega W_s(y),$$
$$W_s(1) = W_c(\pm 1) = 0, \quad W_s(-1) = 1,$$

where $W_r''(y)$ denotes a second derivative of $W_r(y)$, that is $W_r''(y) := \mathrm{d}^2W_r(y)/\mathrm{d}y^2$, $r = s$ or $r = c$. Note that $\Omega := \omega_o R = \omega_w\delta^2/\nu$, with $\omega_w := 2\pi/T_w$, represents the Stokes number. It is a standard fact that the Stokes number quantifies a ratio between: a) diffusive time-scale $T_d := \delta^2/\nu$ and wall oscillation period T_w; b) channel half-width δ and Stokes layer thickness $(\nu/\omega_w)^{1/2}$. Clearly, the solution to the above TPBVP depends only on y and Ω; this dependence can be readily determined symbolically using MATHEMATICA.

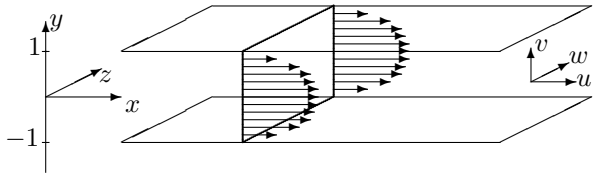

Fig. 1. Three dimensional channel flow.

B. Linearized Navier-Stokes equations

The dynamics of fluctuations around a nominal flow condition $(\bar{\mathbf{u}}, \bar{P})$ are derived by expressing the flow and the forcing fields as the sum of nominal and fluctuation terms $\{\mathbf{u} := \bar{\mathbf{u}} + \mathbf{v},\ P := \bar{P} + p,\ \mathbf{F} := \bar{\mathbf{F}} + \mathbf{d} = \mathbf{d}\}$. If $\bar{\mathbf{u}}$ represents a steady-state solution of the NS equations subject to $(\bar{P}, \bar{\mathbf{F}})$ the linearization of (1) yields

$$\mathbf{v}_t = -\ \bar{\mathbf{u}}\mathbf{v} -\ \mathbf{v}\bar{\mathbf{u}} -\ p + \frac{1}{R}\Delta\mathbf{v} + \mathbf{d}, \tag{4a}$$
$$0 = \ \cdot\mathbf{v}. \tag{4b}$$

These equations govern the dynamics (up to first order) of velocity and pressure fluctuations $\mathbf{v} := \begin{bmatrix} u & v & w \end{bmatrix}^T$ and p in the presence of a body force fluctuation $\mathbf{d} := \begin{bmatrix} d_1 & d_2 & d_3 \end{bmatrix}^T$. This force represents an external excitation to the linearized NS equations (4). On the other hand, nominal velocity $\bar{\mathbf{u}}$ enters as a coefficient into these equations. Each field in (4) is assumed to vary both temporally and spatially, e.g. $\mathbf{d} = \mathbf{d}(x,y,z,t)$.

Since the nominal velocity determines coefficients of the linearized NS equations, system (4) inherits the constant coefficients in x and z, and the *periodic coefficients in time*. Thus, the Fourier transform in x and z can be used to convert the linearized NS equations into a family of PDEs in y with *temporally periodic coefficients*. This family of PDEs is parameterized by the horizontal wave-numbers k_x and k_z, the Reynolds numbers R and R_w, and the Stokes number Ω. By applying a standard conversion to the wall-normal velocity (v)/wall-normal vorticity (η) formulation [14], we transform (4) with $\bar{\mathbf{u}} := \begin{bmatrix} U(y) & 0 & W(y,t) \end{bmatrix}^T$ to

$$\begin{aligned} \boldsymbol{\psi}_t(k_x,y,k_z,t) &= A(k_x,k_z)\,\boldsymbol{\psi}(k_x,y,k_z,t) + \\ &\quad B(k_x,k_z)\,\mathbf{d}(k_x,y,k_z,t), \\ \mathbf{v}(k_x,y,k_z,t) &= C(k_x,k_z)\,\boldsymbol{\psi}(k_x,y,k_z,t), \end{aligned} \tag{5}$$

where $\boldsymbol{\psi} := \begin{bmatrix} v & \eta \end{bmatrix}^T$, and A, B, and C are given by

$$A := \begin{bmatrix} A_{11} & 0 \\ A_{21} & A_{22} \end{bmatrix},\ C := \frac{1}{k^2}\begin{bmatrix} \mathrm{j}k_x\partial_y & -\mathrm{j}k_z \\ k^2 & 0 \\ \mathrm{j}k_z\partial_y & \mathrm{j}k_x \end{bmatrix},$$
$$B := \begin{bmatrix} -\mathrm{j}k_x\Delta^{-1}\partial_y & -k^2\Delta^{-1} & -\mathrm{j}k_z\Delta^{-1}\partial_y \\ \mathrm{j}k_z & 0 & -\mathrm{j}k_x \end{bmatrix},$$
$$A_{11} := \Delta^{-1}\left(\tfrac{1}{R}\Delta^2 + \mathrm{j}k_x\big(U''(y) - U(y)\Delta\big)\right) + \mathrm{j}k_z\Delta^{-1}\big(W''(y,t) - W(y,t)\Delta\big),$$
$$A_{21} := -\mathrm{j}k_z U'(y) + \mathrm{j}k_x W'(y,t),$$
$$A_{22} := (1/R)\Delta - \mathrm{j}k_x U(y) - \mathrm{j}k_z W(y,t),$$
$$W := \frac{2R_w}{R}\big(W_c(y)\cos\,\frac{\Omega t}{R} + W_s(y)\sin\,\frac{\Omega t}{R}\big),$$

with $\mathrm{j} := \sqrt{-1}$ and $k^2 := k_x^2 + k_z^2$. System (5) is subject to the following boundary conditions $\{v(k_x,\pm 1,k_z,t) = v_y(k_x,\pm 1,k_z,t) = \eta(k_x,\pm 1,k_z,t) = 0,\ \forall\ k_x,\ k_z \in \mathbb{R},\ \forall\ t \geq 0\}$, which are derived from the original no-slip boundary conditions on (u,v,w).

III. Frequency response of LTP systems

We next introduce a notion of the *frequency response* for stable LTP systems with period $T = 2\pi/\omega_o$. We refer the reader to [18]–[22] for additional information.

It is a standard fact that a frequency response of a stable linear time-invariant (LTI) system describes how a persistent harmonic input of a certain frequency propagates through the system in the steady-state. In other words, the steady-state response of a stable LTI system to an input signal of frequency ω, is a periodic signal of the same frequency, but with a modified amplitude and phase. The amplitude and phase of the output signal are precisely determined by the value of the frequency response at the input frequency ω.

On the other hand, a steady-state response of a stable LTP system to a harmonic input of frequency θ contains an infinite number of harmonics separated by integer multiplies of ω_o, that is $\theta + n\omega_o$. Using this fact and the analogy with the LTI systems, the frequency response of an LTP system can be defined in terms of *exponentially modulated periodic* (EMP) signals [18]. Namely, the steady-state response of (5) to an

EMP signal

$$\mathbf{d}(k_x, y, k_z, t) \;=\; \sum_{n=-\infty}^{\infty} \mathbf{d}_n(k_x, y, k_z) \mathrm{e}^{\mathrm{j}(n\omega_o + \theta)t},$$

is also an EMP signal

$$\mathbf{v}(k_x, y, k_z, t) \;=\; \sum_{n=-\infty}^{\infty} \mathbf{v}_n(k_x, y, k_z) \mathrm{e}^{\mathrm{j}(n\omega_o + \theta)t},$$

where $\mathbf{d}_n(k_x, y, k_z)$ and $\mathbf{v}_n(k_x, y, k_z)$ are the functions of y parameterized by k_x and k_z, and $\theta \in [0, \omega_o)$ is the angular frequency. The frequency response of (5) is an operator $\mathcal{H}_\theta(k_x, k_z)$ that maps a bi-infinite input vector $\mathrm{col}\,\{\mathbf{d}_n(k_x, y, k_z)\}_{n\,\in\,\mathbb{Z}}$ to a bi-infinite output vector $\mathrm{col}\,\{\mathbf{v}_n(k_x, y, k_z)\}_{n\,\in\,\mathbb{Z}}$.

It can be shown that $\mathcal{H}_\theta(k_x, k_z)$ can be expressed as

$$\mathcal{H}_\theta(k_x, k_z) \;=\; \mathcal{C}(k_x, k_z)(\mathcal{E}(\theta) \;-\; \mathcal{A}(k_x, k_z))^{-1}\mathcal{B}(k_x, k_z),$$

where $\mathcal{E}(\theta)$ is a block-diagonal operator given by $\mathcal{E}(\theta) := \mathrm{diag}\,\{\mathrm{j}(\theta + n\omega_o)I\}_{n\,\in\,\mathbb{Z}}$, and I is the identity operator. On the other hand, $\mathcal{A}$, $\mathcal{B}$, and $\mathcal{C}$ represent block-Toeplitz operators, e.g.

$$\mathcal{A} \;:=\; \mathrm{toep}\,\{\cdots, A_2, A_1, \boxed{A_0}, A_{-1}, A_{-2}, \cdots\},$$

where the box denotes the element on the main diagonal of $\mathcal{A}$. For notational convenience, we suppress the dependence on k_x and k_z here. This bi-infinite matrix representation is obtained by expanding operators A, B, and C in (5) into their Fourier series, e.g. $A(k_x, k_z, t) = \sum_{n=-\infty}^{\infty} A_n(k_x, k_z)\mathrm{e}^{\mathrm{j}n\omega_o t}$. Clearly, since B and C are time-invariant operators their block-Toeplitz representations simplify to block-diagonal representations, i.e. $\mathcal{B}(k_x, k_z) = \mathrm{diag}\,\{B(k_x, k_z)\}$ and $\mathcal{C}(k_x, k_z) = \mathrm{diag}\,\{C(k_x, k_z)\}$.

For each value of (k_x, k_z, θ), $\mathcal{H}_\theta(k_x, k_z)$ is a bi-infinite matrix whose elements are one-dimensional operators in the wall-normal direction. This infinite dimensional object contains a large amount of information about the dynamical properties of system (5). In [16], [17], the frequency responses of the NS equations in channel flows linearized around $U(y)$ were analyzed as the functions of R, k_x, and k_z. The temporal and wall-normal dynamics were aggregated by computing the $\mathcal{H}_2$ norm [23]. At any k_x and k_z the $\mathcal{H}_2$ norm quantifies the variance (energy) amplification of stochastic excitations [17]. Since we are interested in comparing the input-output gains for channel flows with and without spanwise wall oscillations we next define the $\mathcal{H}_2$ norm for LTP system (5):

$$\left[\|\mathcal{H}\|_2^2\right](k_x, k_z) \;:=\; \frac{1}{2\pi}\int_0^{\omega_o} \mathrm{trace}\;(\mathcal{H}_\theta^*(k_x, k_z)\mathcal{H}_\theta(k_x, k_z))\;\mathrm{d}\theta. \tag{6}$$

We note that integration over θ in (6) can be avoided; namely, the $\mathcal{H}_2$ norm of system (5) can be expressed in terms of a solution to the following *harmonic Lyapunov equation* [20]

$$\mathcal{F}(k_x, k_z)\mathcal{V}(k_x, k_z) \;+\; \mathcal{V}(k_x, k_z)\mathcal{F}^*(k_x, k_z) \;=\; -\;\mathcal{B}(k_x, k_z)\mathcal{B}^*(k_x, k_z),$$

as

$$\left[\|\mathcal{H}\|_2^2\right](k_x, k_z) = \mathrm{trace}(\mathcal{V}(k_x, k_z)\mathbf{c}^*(k_x, k_z)\mathbf{c}(k_x, k_z)),$$

where $\mathcal{F}(k_x, k_z) := \mathcal{A}(k_x, k_z) - \mathcal{E}(0)$, and

$$\mathbf{c}(k_x, k_z) \;:=\; \left[\;\cdots \quad 0 \quad C(k_x, k_z) \quad 0 \quad \cdots\;\right].$$

A. Perturbation analysis of the $\mathcal{H}_2$ norm

At any pair of the spatial wave-numbers, the entries into the harmonic Lyapunov equation are bi-infinite operator-valued (in the wall-normal direction) matrices. Thus, a discretization of the linearized NS equations in y in combination with a truncation of bi-infinite matrices would require solving a large-scale Lyapunov equation; for an accurate computation of the $\mathcal{H}_2$ norm the entries into this equation are typically matrices with at least several hundred rows and columns. This is arguably a computationally intensive undertaking. In view of this, we consider a problem of the small wall oscillation amplitudes in this paper. For this special case, we employ a perturbation analysis developed in a companion paper [22]; this analysis provides a computationally efficient method for determining the $\mathcal{H}_2$ norm. Namely, the $\mathcal{H}_2$ norm is obtained by solving a conveniently coupled system of Lyapunov and Sylvester equations. The order of each of these equations is determined by the size of discretization in y.

Proposition 1: The $\mathcal{H}_2$ norm of system (5) with

$$A(t) \;=\; A_0 \;+\; \alpha\left(A_{-1}\mathrm{e}^{-\,\mathrm{j}\omega_o t} \;+\; A_1\mathrm{e}^{\mathrm{j}\omega_o t}\right),$$
$$0 \;<\; \alpha \;=\; R_w/R \;\ll\; 1, \quad \omega_o \;=\; \Omega/R,$$

is given by

$$\|\mathcal{H}\|_2^2 \;=\; \textstyle\sum_{n\,=\,0}^{\infty}\alpha^{2n}\,\mathrm{trace}\;(V_{2n,0}\,C^*C)\,,$$

where

$$A_0V_{0,0} \;+\; V_{0,0}A_0^* \;=\; -\,BB^*,$$
$$A_0V_{2n,0} \;+\; V_{2n,0}A_0^* \;=\; -\,(A_1V_{2n-1,1} \;+\; V_{2n-1,1}^*A_1^* \;+\; A_{-1}V_{2n-1,1}^* \;+\; V_{2n-1,1}A_{-1}^*),$$
$$(A_0 \;+\; \mathrm{j}l\omega_o I)V_{l,l} \;+\; V_{l,l}A_0^* \;=\; -\,(A_{-1}V_{l-1,l-1} \;+\; V_{l-1,l-1}A_1^*), \quad l \;\in\; \mathbb{N},$$
$$(A_0 \;+\; \mathrm{j}m\omega_o I)V_{l,m} \;+\; V_{l,m}A_0^* \;=\; -\,(A_{-1}V_{l-1,m-1} \;+\; V_{l-1,m-1}A_1^* \;+\; A_1V_{l-1,m+1} \;+\; V_{l-1,m+1}A_{-1}^*),$$
$$m \;=\; \begin{cases} 2, 4, \ldots, l-2 & l \;-\; \text{even}, \\ 1, 3, \ldots, l-2 & l \;-\; \text{odd}. \end{cases}$$

Proposition 1 clarifies the dependence of the energy amplification on wall oscillation amplitude α, $0 < \alpha \ll 1$. Since the operators appearing in the expression for the $\mathcal{H}_2$ norm depend on the wave-numbers k_x and k_z, the Reynolds number R, and the Stokes number Ω, the energy amplification is also a function of these parameters. In § IV, we derive an explicit scaling of the $\mathcal{H}_2$ norm with R for system (5) at $k_x = 0$, and analyze the changes in energy amplification with k_z and Ω. All numerical computations are performed using a Matlab Differentiation Matrix Suite [24] with 50 collocation points in y.

IV. Energy amplification at $k_x = 0$

In this section, we study system (5) in the important special case of streamwise constant three-dimensional per-

turbations. The motivation for a thorough analysis of this model stems from the fact that the streamwise constant perturbations in channel flows experience largest stochastic amplification rates [15]–[17]. Our objective is to quantify the influence of small-amplitude transverse wall oscillations on these amplification rates. We employ a perturbation analysis to derive an explicit dependence of the $\mathcal{H}_2$ norm on the Reynolds number. We also study the $\mathcal{H}_2$ norm as a function of k_z and Ω, and identify the values of the Stokes number that lead to the $\mathcal{H}_2$ norm reduction.

We show that suppression (enhancement) of turbulence by transverse wall oscillations is due to decreased (increased) variance amplification compared to the uncontrolled flow. In other words, the wall oscillation induced changes in nominal velocity constrain velocity perturbations to experience smaller (for suppression of turbulence) or larger (for enhancement of turbulence) stochastic amplification rates [25]. In the language of control theory, the influence of transverse wall oscillations is quantified by the $\mathcal{H}_2$ norm of operator that maps the external excitations to the velocity perturbations. The turbulence suppression takes place if the $\mathcal{H}_2$ norm of controlled system is reduced compared to the $\mathcal{H}_2$ norm of the uncontrolled system. The system norms were previously employed by Farrell & Ioannou [25] and Kim [26] for evaluation of active flow control strategies. However, to the best of the author's knowledge this approach has not been used for assessing effectiveness of sensorless flow control strategies.

By setting $k_x = 0$ in (5) we obtain

$$\begin{aligned} \boldsymbol{\psi}_t(y,k_z,t) &= A(k_z,t)\,\boldsymbol{\psi}(y,k_z,t) + B(k_z)\,\mathbf{d}(y,k_z,t),\\ \mathbf{v}(y,k_z,t) &= C(k_z)\,\boldsymbol{\psi}(y,k_z,t), \end{aligned} \tag{7}$$

where, for

$$W(y,t) \;=\; (2R_w/R)(W_c(y)\cos\tfrac{\Omega t}{R} \;+\; W_s(y)\sin\tfrac{\Omega t}{R}),$$

we have

$$A(k_z,t) = A_0(k_z) + \tfrac{R_w}{R}(A_{-1}(k_z)\mathrm{e}^{-\,\mathrm{j}\frac{\Omega t}{R}} + A_1(k_z)\mathrm{e}^{\mathrm{j}\frac{\Omega t}{R}}),$$

with $A_{\pm1}(k_z) := A_c(k_z) \mp \mathrm{j}A_s(k_z)$, and

$$\begin{aligned} A_0(k_z) &:= \begin{bmatrix} \frac{1}{R}L_0(k_z) & 0 \\ C_{p0}(k_z) & \frac{1}{R}S_0(k_z) \end{bmatrix},\\ A_{\pm1}(k_z) &:= \begin{bmatrix} L_{\pm1}(k_z) & 0 \\ 0 & S_{\pm1}(k_z) \end{bmatrix},\\ L_{\pm1}(k_z) &:= L_c(k_z) \mp \mathrm{j}L_s(k_z),\\ S_{\pm1}(k_z) &:= S_c(k_z) \mp \mathrm{j}S_s(k_z). \end{aligned}$$

The underlying operators in $A_0(k_z)$ and $A_r(k_z)$, for $r = c$ or $r = s$, are determined by

$$\begin{aligned} L_0 &:= \Delta^{-1}\Delta^2,\quad C_{p0} := -\mathrm{j}k_zU'(y),\\ S_0 &:= \Delta,\quad S_r := -\mathrm{j}k_zW_r(y),\\ L_r &:= \mathrm{j}k_z\Delta^{-1}\big(W_r''(y) - W_r(y)\Delta\big), \end{aligned}$$

where $\Delta := \partial_{yy} - k_z^2$, with homogenous Dirichlet boundary conditions, and $\Delta^2 := \partial_{yyyy} - 2k_z^2\partial_{yy} + k_z^4$, with homogenous Dirichlet *and* Neumann boundary conditions. It is a standard fact that, for any (k_z,R), $A_0(k_z)$ represents an exponentially stable operator [14]. We also note that $B(k_z)B^*(k_z) = I$ and $C^*(k_z)C(k_z) = I$, which is important for the $\mathcal{H}_2$ norm computations (see [17] for details).

We next state the result that quantifies energy amplification of streamwise constant perturbations in parallel channel flows subject to small amplitude transverse wall oscillations. The proof of Theorem 2 is given in Appendix A.

Theorem 2: For any parallel channel flow $U(y)$ subject to small amplitude transverse wall oscillations

$$W(y=-1,t) \;=\; 2(R_w/R)\sin(\Omega/R)t,\quad R_w \ll R,$$

the energy amplification of streamwise constant perturbations is given by

$$\begin{aligned} \big[\|\mathcal{H}\|_2^2\big](k_z) \;=\; &\big(f_0(k_z) + \textstyle\sum_{n=1}^{\infty} R_w^{2n}\, f_{2n}(k_z,\Omega)\big)\,R \;+\\ &\big(g_0(k_z) + \textstyle\sum_{n=1}^{\infty} R_w^{2n}\, g_{2n}(k_z,\Omega)\big)\,R^3. \end{aligned}$$

Theorem 2 establishes an explicit scaling of the energy amplification with the Reynolds numbers R and R_w for *any* streamwise constant parallel channel flow subject to small amplitude transverse wall oscillations. As shown in Appendix A, functions f and g in Theorem 2 represent traces of the solutions to certain operator Lyapunov equations, and the f functions do not depend on $U(y)$. Thus, $f_0(k_z)$ and $f_{2n}(k_z,\Omega)$ are the same for *all* parallel channel flows $U(y)$. On the other hand, $g_0(k_z)$ and $g_{2n}(k_z,\Omega)$ depend on the underlying parallel flow through their dependence on the nominal shear $U'(y)$. Since a contribution of g_0 and g_{2n} to the $\mathcal{H}_2$ norm scales as R^3, these two functions play a dominant role in the amplification of stochastic excitations for the large-Reynolds-number channel flows.

In the absence of wall oscillations (that is, at $R_w = 0$), we recover a formula for the $\mathcal{H}_2$ norm of the streamwise constant NS equations linearized around $U(y)$ [15]. Functions f_0 and g_0 are thoroughly analyzed in [15]–[17]; for completeness, they are also shown in the first row of Fig. 2. The peak in the plot of g_0 determines the most energetic structures in the velocity field excited by a broad-band, stochastic input field $\mathbf{d}$. In Poiseuille flow this peak takes place at $k_z \approx 1.78$. As the plot of g_2 reveals, the Stokes number Ω determines whether transverse oscillations amplify or attenuate the most energetic components of the uncontrolled flow. We observe that the largest attenuation occurs at $\bar{\Omega} \approx 17.61$. Since the influence of f_2 on the energy amplification at large Reynolds numbers is negligible compared to the influence of g_2 (R vs. R^3 scaling), $\bar{\Omega}$ represents the Stokes number that provides the largest $\mathcal{H}_2$ norm reduction (up to a second order in parameter R_w). Note that the largest negative contributions of g_2 to the energy amplification are located in the region of k_z's where function g_0 peaks; this indicates that the spanwise wall oscillations introduce interactions with the most energetic modes (streamwise vortices and streaks) of the uncontrolled flow which leads to a parametric resonance.

The (k_z,Ω)–dependence of functions g_4, g_6, g_8, and g_{10} in Poiseuille flow is shown in Fig. 3. These plots indicate a progressive decrease in the magnitude of higher order corrections to the $\mathcal{H}_2$ norm. For the values of Ω where g_2 provides the largest energy amplification reduction, there is an alternating positive and negative contribution of the higher order corrections to the $\mathcal{H}_2$ norm.

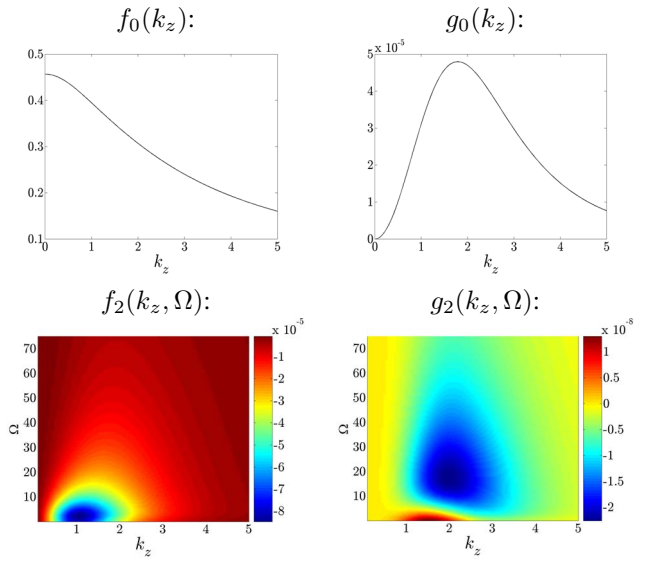

Fig. 2. Plots of functions f_0, g_0, f_2, and g_2 in Theorem 2. The g-functions are shown in Poiseuille flow.

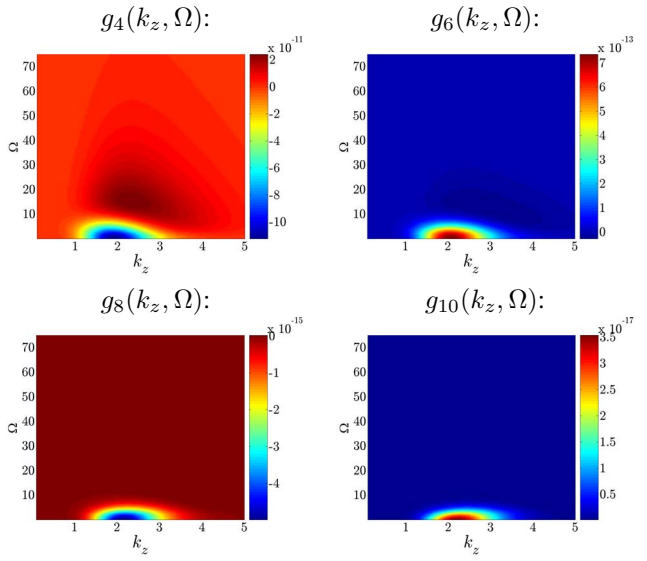

Fig. 3. Plots of functions g_4, g_6, g_8, and g_{10} in Poiseuille flow.

The plots of Fig. 4 suggest inherent limitations (i.e., the slow convergence and the lack of convergence) of the perturbation analysis for large wall oscillation amplitudes. Despite these limitations the perturbation analysis is capable of identifying important trends in amplification of ambient disturbances. In particular, our method provides a paradigm for the optimal selection of transverse oscillation frequencies for turbulence suppression. When the frequency is selected, the large-scale computations can be used to determine the energy amplification even for oscillation amplitudes at which perturbation analysis fails to converge. This is illustrated in Fig. 5 where the $\mathcal{H}_2$ norms of uncontrolled Poiseuille with $R = 2000$ (blue), and controlled Poiseuille with $\{R = 2000,\ R_w = 20,\ \Omega = 17.61\}$ (green) and $\{R = 2000,\ R_w = 50,\ \Omega = 17.61\}$ (red) are shown. The green curve is obtained by approximating the infinite summations in the expression for $\left[\|\mathcal{H}\|_2^2\right](k_z)$ by summations with five terms, and it closely matches the results obtained using large-scale computations. On the other hand, the red curve is obtained using large-scale computations. Thus, *properly designed* transverse wall oscillations with amplitudes equal to $2\,\%$ and $5\,\%$ of the maximal nominal velocity ($R_w/R = 0.01$ and $R_w/R = 0.025$, respectively), reduce the largest energy amplification of the uncontrolled Poiseuille flow by approximately $14\,\%$ and $35\,\%$. This demonstrates the ability of transverse wall oscillations to significantly weaken the most energetic structures in transitional channel flows.

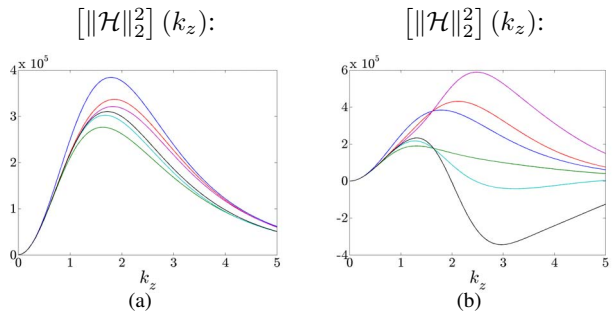

Fig. 4. The $\mathcal{H}_2$ norms of Poiseuille flow with $R = 2000$, and: (a) $\{R_w = 25,\ \Omega = 17.61\}$; (b) $\{R_w = 35,\ \Omega = 17.61\}$. The blue curves denote the uncontrolled flow; the controlled flow plots are obtained using Theorem 2 with the infinite sums approximated by the sums with: 1 (green), 2 (red), 3 (cyan), 4 (magenta), and 5 (black) terms. As shown in plot (b), the perturbation analysis fails to converge for large values of R_w.

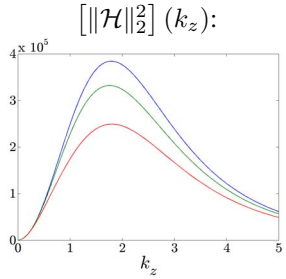

Fig. 5. The energy amplification of uncontrolled Poiseuille flow with $R = 2000$ (blue), and controlled Poiseuille flow with $\{R = 2000,\ R_w = 20,\ \Omega = 17.61\}$ (green) and $\{R = 2000,\ R_w = 50,\ \Omega = 17.61\}$ (red).

Our results show that the transverse wall oscillations of appropriate frequency have a potential for reducing the energy amplification of streamwise constant perturbation which consequently leads to a smaller turbulence production [13], [25].

V. Concluding Remarks

This paper develops a system theoretic paradigm for modeling, optimization, and evaluation of sensorless flow control strategies in wall-bounded shear flows. The new paradigm represents a spatio-temporal analog of the well-known principle of *vibrational control*, where the system's dynamical properties are altered by introducing zero-mean vibrations into the system's coefficients [27]. Depending on the relationship between the natural modes of the uncontrolled system and the forcing frequency, the vibrational control may have a potential for providing stability of the overall system and for changing its input-output norms. For example, it is well known that the inverted pendulum

can be stabilized by sensorless means using high frequency oscillations of the suspension point [27]. We show that the principle of vibrational control can be also utilized in systems governing the dynamics of flow fluctuations in channel flows, where coefficients multiplying system's state have temporal periodicity. The key observation is that there is a potential for changing dynamical properties of the NS equations (in favorable or unfavorable manner) whenever temporal (or spatial) vibrations enter into the system's coefficients.

We model and analyze the influence of small amplitude transverse wall oscillations on energy amplification in channel flows. We develop models that govern the dynamics of flow fluctuations; the transverse oscillation parameters enter as coefficients, and the body force fields enter as stochastic excitations into these models. We conduct a robustness analysis for the derived models, which yields optimal oscillation frequency (as a function of the Reynolds number) for turbulence suppression. Our results provide a first compelling theoretical explanation as to why *properly designed* transverse wall oscillations can suppress turbulence in channel flows.

APPENDIX

A. Proof of Theorem 2

We next use Proposition 1 to clarify the dependence of the $\mathcal{H}_2$ norm of system (7) with $\{W(y,t) = 2\alpha\,(W_c(y)\cos\omega_o t + W_s(y)\sin\omega_o t)\,;\ \alpha = R_w/R,\ \omega_o = \Omega/R\}$ on R, Ω, and k_z; our derivations are summarized in Theorem 2.

Since $W_c(y)$ and $W_s(y)$ are parameterized by the Stokes number, $\Omega := \omega_o R$, we represent operator $F(n) := A_0 - \mathrm{j}n(\Omega/R)I$ as

$$F(n) \;=\; \left[\begin{array}{cc} \frac{1}{R}(L_0 - \mathrm{j}n\Omega I) & 0 \\ C_{p0} & \frac{1}{R}(S_0 - \mathrm{j}n\Omega I) \end{array}\right].$$

By decomposing $V_{l,k}$ into 2×2 operator-blocks

$$\begin{array}{rcl} V_{l,m} & := & R^l \left[\begin{array}{cc} R\,X_{l,m} & R^2\,\Pi_{l,m} \\ R^2\,Y_{l,m} & R\,Z_{l,m_a} + R^3\,Z_{l,m_b} \end{array}\right], \\ m & = & \left\{\begin{array}{lll} 0,2,\ldots,l & l & - \ \text{even}, \\ 1,3,\ldots,l & l & - \ \text{odd}, \end{array}\right. \\ X^*_{2n,0} & = & X_{2n,0},\ \ \Pi_{2n,0} \;=\; Y^*_{2n,0}, \\ Z^*_{2n,0_{(\,)}} & = & Z_{2n,0_{(\,)}},\ \ n\in\mathbb{N}_0, \end{array}$$

we can use Proposition 1 to derive a system of conveniently coupled Reynolds-number-independent equations for $X_{l,m}$, $Y_{l,m}$, $\Pi_{l,m}$, Z_{l,m_a}, and Z_{l,m_b}. Due to page constraints, these equations are not reported here.

Now, we combine Proposition 1 and the above derivations with $C^*C = I$ to obtain

$$\begin{array}{l} \|\mathcal{H}\|_2^2 \;=\; \mathrm{trace}\,\left(R(X_{0,0} + Z_{0,0_a}) + R^3 Z_{0,0_b}\right) + \\ \sum_{n=1}^{\infty}(\alpha R)^{2n}\,\mathrm{trace}\,\left(R(X_{2n,0} + Z_{2n,0_a}) + R^3 Z_{2n,0_b}\right). \end{array}$$

Furthermore, since $\{X_{0,0}, Z_{0,0_a}, Z_{0,0_b}\}$ and $\{X_{2n,0},\ Z_{2n,0_a},\ Z_{2n,0_b};\ n\in\mathbb{N}\}$ depend on k_z and (k_z,Ω), respectively, the expression for the $\mathcal{H}_2$ norm of (7) can be rewritten as

$$\begin{array}{rcl} \left[\|\mathcal{H}\|_2^2\right](k_z) & = & (f_0(k_z) + \sum_{n=1}^{\infty} R_w^{2n}\, f_{2n}(k_z,\Omega))R + \\ & & (g_0(k_z) + \sum_{n=1}^{\infty} R_w^{2n}\, g_{2n}(k_z,\Omega))R^3, \end{array}$$

where $\{f_{2n} := \mathrm{trace}\,(X_{2n,0}) + \mathrm{trace}\,(Z_{2n,0_a}),\ g_{2n} := \mathrm{trace}\,(Z_{2n,0_b}),\ n\in\mathbb{N}_0\}$. This proves Theorem 2.

REFERENCES

[1] W. Jung, N. Mangiavacchi, and R. Akhavan, "Suppression of turbulence in wall-bounded flows by high-frequency spanwise oscillations," *Phys. Fluids A*, vol. 4, no. 8, pp. 1605–1607, 1992.

[2] A. Baron and M. Quadrio, "Turbulent drag reduction by spanwise wall oscillations," *Appl. Sci. Res.*, vol. 55, no. 4, pp. 311–326, 1996.

[3] T. W. Berger, J. Kim, C. Lee, and J. Lim, "Turbulent boundary layer control utilizing the Lorentz force," *Phys. Fluids*, vol. 12, no. 3, pp. 631–649, 2000.

[4] M. Quadrio and P. Ricco, "Critical assessment of turbulent drag reduction through spanwise wall oscillations," *J. Fluid Mech.*, vol. 521, pp. 251–271, 2004.

[5] P. Orlandi and M. Fatica, "Direct simulations of turbulent flow in a pipe rotating about its axis," *J. Fluid Mech.*, vol. 343, pp. 43–72, 1997.

[6] K.-S. Choi and M. Graham, "Drag reduction of turbulent pipe flows by circular-wall oscillation," *Phys. Fluids*, vol. 10, no. 1, pp. 7–9, 1998.

[7] M. Quadrio and S. Sibilla, "Numerical simulation of turbulent flow in a pipe oscillating around its axis," *J. Fluid Mech.*, vol. 424, pp. 217–241, 2000.

[8] F. Laadhari, L. Skandaji, and R. Morel, "Turbulence reduction in a boundary layer by a local spanwise oscillating surface," *Phys. Fluids*, vol. 6, no. 10, pp. 3218–3220, 1994.

[9] K.-S. Choi, J.-R. DeBisschop, and B. R. Clayton, "Turbulent boundary-layer control by means of spanwise-wall oscillation," *AIAA J.*, vol. 36, no. 7, pp. 1157–1163, 1998.

[10] K.-S. Choi, "Near-wall structure of turbulent boundary layer with spanwise-wall oscillation," *Phys. Fluids*, vol. 14, no. 7, pp. 2530–2542, 2002.

[11] K. M. Butler and B. F. Farrell, "Three-dimensional optimal perturbations in viscous shear flow," *Phys. Fluids A*, vol. 4, p. 1637, 1992.

[12] L. N. Trefethen, A. E. Trefethen, S. C. Reddy, and T. A. Driscoll, "Hydrodynamic stability without eigenvalues," *Science*, vol. 261, pp. 578–584, 1993.

[13] B. F. Farrell and P. J. Ioannou, "Stochastic forcing of the linearized Navier-Stokes equations," *Phys. Fluids A*, vol. 5, no. 11, pp. 2600–2609, 1993.

[14] P. J. Schmid and D. S. Henningson, *Stability and Transition in Shear Flows*. New York: Springer-Verlag, 2001.

[15] B. Bamieh and M. Dahleh, "Energy amplification in channel flows with stochastic excitation," *Phys. Fluids*, vol. 13, no. 11, pp. 3258–3269, 2001.

[16] M. R. Jovanović, "Modeling, analysis, and control of spatially distributed systems," Ph.D. dissertation, University of California, Santa Barbara, 2004.

[17] M. R. Jovanović and B. Bamieh, "Componentwise energy amplification in channel flows," *J. Fluid Mech.*, vol. 534, pp. 145–183, July 2005.

[18] N. M. Wereley and S. R. Hall, "Frequency response of linear time periodic systems," in *Proceedings of the 29th IEEE Conference on Decision and Control*, Honolulu, HI, 1990, pp. 3650–3655.

[19] J. Zhou and T. Hagiwara, "Existence conditions and properties of the frequency response operators of continuous-time periodic systems," *SIAM J. Control Optim.*, vol. 40, no. 6, pp. 1867–1887, 2002.

[20] J. Zhou, T. Hagiwara, and M. Araki, "Trace formula of linear continuous-time periodic systems via the harmonic Lyapunov equation," *Int. J. Control*, vol. 76, no. 5, pp. 488–500, 2003.

[21] H. Sandberg, "Model reduction for linear time-varying systems," Ph.D. dissertation, Department of Automatic Control, Lund Institute of Technology, Sweden, December 2004.

[22] M. R. Jovanović, "H_2 norm of linear time-periodic systems: a perturbation analysis," in *Proceedings of the 2006 American Control Conference*, Minneapolis, MN, 2006.

[23] K. Zhou, J. C. Doyle, and K. Glover, *Robust and Optimal Control*. Prentice Hall, 1996.

[24] J. A. C. Weideman and S. C. Reddy, "A MATLAB differentiation matrix suite," *ACM Transactions on Mathematical Software*, vol. 26, no. 4, pp. 465–519, December 2000.

[25] B. F. Farrell and P. J. Ioannou, "Turbulence suppression by active control," *Phys. Fluids*, vol. 8, no. 5, pp. 1257–1268, 1996.

[26] J. Kim, "Control of turbulent boundary layers," *Phys. Fluids*, vol. 15, no. 5, pp. 1093–1105, 2003.

[27] S. M. Meerkov, "Principle of vibrational control: theory and applications," *IEEE Trans. Autom. Control*, vol. AC-25, no. 4, pp. 755–762, 1980.